Published in final edited form as:

Med Image Comput Comput Assist Interv. 2019 October ; 11768: 345–353. doi:10.1007/978-3-030-32254-0_39.

An Automatic Approach to Reestablish Final Dental Occlusion for 1-Piece Maxillary Orthognathic Surgery

Han Deng[1,*], **Peng Yuan**[1,*], **Sonny Wong**[2], **Jaime Gateno**[1,3], **Fred A. Garrett**[2], **Randy K. Ellis**[2], **Jeryl D. English**[2], **Helder B. Jacob**[2], **Daeseung Kim**[1], **James J. Xia**[1,3,✉]

[1]Department of Oral and Maxillofacial Surgery, Houston Methodist Research Institute, TX

[2]Department of Orthodontics, University of Texas Houston Health Science Center Dentistry School, TX

[3]Department of Surgery (Oral and Maxillofacial Surgery), Weill Medical College, Cornell University, New York, NY

Abstract

Accurately establishing a desired final dental occlusion of the upper and lower teeth is a critical step in orthognathic surgical planning. Traditionally, the final occlusion is established by hand-articulating the stone dental models. However, this process is inappropriate to digitally plan the orthognathic surgery using computer-aided surgical simulation. To date, there is no effective method of digitally establishing final occlusion. We propose a 3-stage approach to digitally and automatically establish a desired final dental occlusion for 1-piece maxillary orthognathic surgery, including: 1) to automatically extract points of interest and four key teeth landmarks from the occlusal surfaces; 2) to align the upper and lower teeth to a clinically desired Midline-Canine-Molar relationship by minimization of sum of distances between them; and 3) to finely align the upper and lower teeth to a maximum contact with the constraints of collision and clinical criteria. The proposed method was evaluated qualitatively and quantitatively and proved to be effective and accurate.

1 Introduction

Dentistry is going digital, and so is orthognathic surgery. In the last decade, computer-aided surgical simulation (CASS) becomes the standard of care for planning orthognathic surgery.[1] An important step in CASS orthognathic surgery planning is to establish a desired dental occlusion (called "final occlusion") between the upper and lower teeth. Traditionally, surgeons hand-articulate upper and lower stone dental models. The instant tactile response and cognitive insight help them to quickly achieve a desired position of the stone models, i.e., midline alignment, Class I canine and molar relations, and a maximized contact between the upper and lower teeth. However, it is completely different in the digital world. The digital upper and lower dental models are represented by point clouds or triangulated surfaces that have a lack of tactile response. When they are in contact, they can still be

✉ jxia@houstonmethodist.org.
*Contribute Equally

moved towards and penetrate into each other. Therefore, in the current CASS clinical protocol, surgeons still need to hand-articulate the stone models to the final occlusion and use CBCT scanner to scan them together into the computer. It takes at least an hour in the office. If the digital dental models are generated using an intraoral scanner, it will take additional 4 hours to 3D print the teeth models for hand articulation. This process is convoluted, time-consuming and cost-inefficient, and may introduce unpredicted inaccuracy into the planning.

There are reports on digital dental occlusion.[2, 3] However, they either require moving the models together manually or are computationally inefficient, and thus have not been used clinically. In the past, we have developed a method of digitally articulating the upper and lower dental models into maximum intercuspation (MI).[4–6] However, this method is problematic and only used in the laboratory setting. It only considers MI relationship, which is an occlusion that simply maximizes the contacting areas between the upper and lower teeth without considering the other important clinical criteria. Thus, most of time, the results cannot be used in clinical practice. In addition, it requires manually extracting the occlusal surface by removing the braces and the gums from the digital models. Moreover, it is computationally inefficient. Even after the models are manually prepared, it takes more than an hour to complete the computation. Due to these problems, we can only utilize it in the laboratory.

In this project, we propose a three-stage approach to automatically articulate the upper and lower dental models to the final occlusion for 1-piece maxillary orthognathic surgery. In the first stage, points of interest (POI) and four key teeth landmarks (each landmark appears on both left and right side) are automatically extracted from the teeth occlusal surfaces. In the second stage, the upper and lower teeth are aligned to a clinically desired Midline-Canine-Molar (M-C-M) relationship. In the third stage, the upper and lower teeth are finely aligned to a best possible maximum contact, i.e., the best option among many possibilities of making contacts between the upper and lower teeth with the constraints of clinical criteria and collision.

The contributions of this proposed approach are that: 1) the approach jointly considers the clinical criteria and a maximized contact between the upper and lower teeth to seek the best possible final dental occlusion; 2) it is a fully automatic approach without labor-intensive manual manipulation, which is a mandatory step in our previous method; and 3) it is computationally efficient.

2 Method

Our automatic dental articulation is completed in three stages to: 1) extract POI and four key landmarks that are not digitized in regular clinical routine, 2) establish a clinically desired M-C-M relationship, and 3) seek a maximum contact with the constraints of collision and clinical criteria. During the articulation, the lower teeth remains static while the upper teeth articulates onto the lower teeth. Since the digital articulation is a part of CASS planning, all the teeth landmarks, except four, have already been digitized following the clinical routine. [7, 8] Our approach is described below in details.

2.1 POI extraction

Each dental model consists of thousands of points. During the articulation, only the points on the upper and lower occlusal surfaces are occluded. We refer the points on the occlusal surfaces that form the edges, cusps and grooves as POI – the points of interest. They are automatically extracted in the following four steps.

Occlusal surface extraction: Orthodontic braces and gums interfere with the digital dental articulation. Therefore, it is necessary to extract the occlusal surfaces from the teeth models. First, a 200-point fitting curve is created using seven already digitized teeth landmarks (Fig. 1a, Table 1). A plane (called PCA plane) is created by principle component analysis (PCA) using the same landmarks. The distance h_v between each vertex v on the model and the PCA plane is calculated. Then, the fitting curve and the vertices of the entire teeth model are projected onto the PCA plane. The distance r_v between each projected vertex and the projected fitting curve is calculated. We set a threshold H empirically, e.g., 15, since the height of the tooth crown is usually within 10 mm. For each vertex u belongs to model vertex set $\{v\}$ such that $h_u < H$, we define a parameter ϕ_u as $\alpha \cdot h_u + (1 - \alpha) \cdot r_u$, where α is coefficient (empirically set as 0.2) that controls the relative influence of h_u and r_u. Then k-means clustering algorithm is performed using ϕ_u to extract a “clean” surface for the next step (Fig. 1b).

Envelope simplification: A cross-sectional plane of the teeth is created for each point of the fitting curve (Fig. 1c), forming 200 planes for the entire teeth model. An envelope is calculated based on the intersectional line of each cross-sectional plane and the occlusal surface (brown curve in Fig. 1c). Each envelop is then simplified using Douglas-Peucker algorithm to extract key geometric feature points. As shown in Fig. 1d, a line segment is iteratively formed by connecting the two neighboring “keep” points on the envelope. In the first iteration, the two neighboring “keep” points are the start and end points (in purple) of the envelope. Between the two neighboring “keep” points, we search for a point along the envelope that has the largest distance to the line segment, and mark it as a “keep” point (in gray) if the distance is larger than a threshold, e.g., 0.02 mm. Fig. 1d shows the first two iterations.

POI classification: Each “keep” point (in gray in Fig. 1e) is further classified as a “convex point” (in red) if it is in the convex region of the envelope, or a “concave point” (in green) if it is in the concave region. This is done by calculating the concavity of each “keep” point based on Javis’ algorithm. All envelopes are separated into multiple segments by the concave points (Fig.1f). The cusps (in red) are first identified on each segment (Fig. 1g, only showing the buccal cusps). The central groove (in green) is then identified on the segment between the buccal and palatal/lingual cusps (Fig. 1h).

Landmark Detection: The classified cusp points are used together with the already digitized landmarks to detect two pairs of un-digitized but required landmarks for the upper and lower teeth, respectively (Table 1). The distances between each cusp point and the PCA plane are calculated, which are used to seek peaks and valleys among the cusp points (in red, Fig 1g). Finally, the names and the locations of already digitized landmarks are used in conjunction to extract our desired peak and valley points for upper (U6MLC and U56Embr, Fig. 1i) and lower (L6DBC and L34Embr, Fig. 1j) teeth.

2.2 Midline-Canine-Molar alignment

The purpose of M-C-M alignment is to align the "mobile" upper teeth to the "static" lower teeth based on the clinical criteria. The detailed process is described below.

Local Coordinate System.—In order to incorporate the clinical criteria (dental midline alignment, and canine and molar relationships) into the algorithm, a local coordinate system is established for each of the key landmarks on the "static" lower teeth, respectively (Table 1, Fig. 2). First, the lower occlusal plane is created using PCA based on the nine key teeth landmarks. The direction of the normal vector $\boldsymbol{Z}$ of the lower occlusal plane is from the teeth root towards the crown. Next, each landmark is projected to the lower occlusal plane. A new fitting curve is then formed based on the projected landmarks. The local coordinate system is defined as follows: the z-axis for all the landmarks is the normal vector $\boldsymbol{Z}$; the x-axis for each landmark is the tangent line of the fitting curve, pointing from the left side to the right; and the y-axis is orthogonal to the x- and z-axis, pointing from the labial/buccal side to the lingual (Fig. 2c).

Minimization of sum of distances.—In this step, we jointly consider the clinical requirements on midline, canine, and molar. Each upper landmark l_u has a corresponding lower landmark l_l. We rotate and translate upper teeth using a transformation matrix M. Thus, each upper dental landmark l_r has a new position $M \cdot l_r$. The following distances between the paired upper and lower landmarks are calculated: (1) d_{mi}^{x} is the distance between midline landmarks (U0 and L0) along local x-axis, where $\boldsymbol{d_{mi}}$ is a vector from L0 to U0; (2) d_c^x is the distance between each pair of canine landmarks (U3C and L34Embr) along local x-axis, where $\boldsymbol{d_c}$ is a vector from L34Embr to U3C; and (3) d_{mo}^{E} is the *Euclidean* distance between each pair of the molar landmarks (U56Embr and L6MBC, U6MLC and L6CF, U6CF and L6DBC), where $\boldsymbol{d_{mo}}$ is the vector from lower molar landmark to the corresponding upper molar landmark.

It is also important to ensure the upper dental arch is on the labial/buccal side (outside) of the lower dental arch. To ensure that the directions of both vectors $\boldsymbol{d_{mi}}$ and $\boldsymbol{d_c}$ are from the lingual to the labial side, we need $\boldsymbol{y_{mi}} \cdot \boldsymbol{d_{mi}} < 0$ and $\boldsymbol{y_c} \cdot \boldsymbol{d_c} < \boldsymbol{0}$, where $\boldsymbol{y_{mi}}$ and $\boldsymbol{y_c}$ are the local y-axis of L0 and L34Embr, respectively. Similarly, we use $\boldsymbol{d_{mo}}$ to ensure the upper molar is above the lower molar by $\mathbf{z} \cdot \boldsymbol{d_{mo}} > \mathbf{0}$ where z is the local z-axis. In order to apply the above constraints, we add a penalty function by using a large coefficient Ω ($\Omega \to \infty$) for $\boldsymbol{d_{mi}}$, $\boldsymbol{d_c}$, and $\boldsymbol{d_{mo}}$. Thus, the objective function for finding the transformation matrix M of the upper teeth is:

$$Min\left\{d_{mi}^{x} + \sum_{canine} d_{c}^{x} + \sum_{molar} d_{mo}^{E} + \Omega \left[\mathbb{1}(\boldsymbol{y}_{\boldsymbol{mi}} \cdot \boldsymbol{d}_{\boldsymbol{mi}}) + \sum_{canine} \mathbb{1}(\boldsymbol{y}_{\boldsymbol{c}} \cdot \boldsymbol{d}_{\boldsymbol{c}}) + \sum_{molar} \mathbb{1}(-z \cdot \boldsymbol{d}_{\boldsymbol{mo}})\right]\right\}, \tag{1}$$

where $\mathbb{1}$ is indicator function so that $\mathbb{1}(x) := \begin{cases} 1, & if\ x > 0 \\ 0, & if\ x \le 0 \end{cases}$.

2.3 Fine alignment

The purpose of the third stage is to iteratively seek a maximum contact between the upper and lower teeth, while keeping the constraints of collision and clinical criteria (the M-C-M relationship). The details are described below.

Upper and lower POI match.—Clinically, the upper and lower posterior teeth should maintain a tight cusp-fossa intercuspation relationship, while the anterior teeth should make a maximum contacts. Let $\{u_i\}$ and $\{l_j\}$ be the vertices sets of the upper and the lower POIs (the red peak and green valley points in Fig. 1g and 1h), respectively. Each u_i is paired with a lower POI l_{j_i} by finding the vertex with the closest distance to u_i, i.e., $l_{j_i} = argmin_{l\epsilon\{l_j\}} \| u_i - l \|$. The goal is to minimize the overall distance between $\{u_i\}$ and $\{l_{j_i}\}$.

Collison constraint.—The upper and lower teeth should not penetrate into each other. Therefore, the collision is constrained by the penetration depth between occlusal surfaces of the upper and lower teeth. Based on our clinical observation, a 0.1mm of penetration depth is allowed because it is deemed to be an error of the constructed STL model. The upper and lower vertices on occlusal surfaces are paired using the same method for point match. For each pair, the penetration depth is calculated as the distance of upper vertex v_{upper} and lower vertex v_{lower} along the normal direction of the lower vertex $\boldsymbol{n}_{lower}$. They should not be greater than 0.1 mm. In addition, to reduce the computational complexity, we only compute the penetration depth when the Euclidean distance between a pair of vertices is smaller than a certain threshold ϵ, i.e., 1.0 mm. The constraint is $(Rv_{upper} + t - v_{lower}) \cdot \boldsymbol{n}_{lower} + \epsilon \ge 0$, where R is rotation matrix and t is translation matrix.

Clinical criteria constraint.—During the POI-based fine alignment, the M-C-M relationship must be maintained. Therefore, we set a threshold for constraining the distances between the landmarks U0 and L0 along the local x,y, and z-axes (Fig. 2c). The movement and resulted position of U0 is constrained by the clinical criteria and normative values, i.e., the distance along the x-axis is within 1.5 mm for midline deviation; the distance along the y-axis is within the normal range of 1.5-3.0 mm for overjet; and the distance along the z-axis is within the normal range of 2.0-4.0 mm for overbite (the deeper the better). We believe that such a small amount of the movement will not disrupt the canine and molar relationships established by M-C-M alignment.

Transformation matrix update.—During each iteration, a rotational center of the upper teeth model is calculated and updated based on the distance between the upper and the lower

POIs. A weight is assigned to each vertex on the upper POI according to its distance to the closest vertex on the lower POI as $w_i = \frac{1}{e^{|u_i - l_{j_i}|}}$. The rotation center is calculated as weighted center of upper POI, i.e., $\tilde{o} \leftarrow \frac{\sum_i w_i u_i}{\sum_i w_i}$.

The transformation of the upper teeth is calculated by solving the optimization problem of minimizing the distance between current paired $\{u_i\}$ and $\{l_{j_i}\}$ subject to the above collision and clinical constraints. The objective function is written as

$$Min \sum_{i=1}^{n} \left\| R\left(u_i - \tilde{o}\right) + \tilde{o} + t - l_{j_i} \right\|^2 \quad (2)$$

where R is rotation matrix and t is translation matrix.

The upper teeth model is thus translated and rotated to a new position. In the following iteration, we re-match upper and lower POI and repeat the above steps. The process is stopped when the difference between overall distances yield from two consecutive iterations is small than a certain threshold δ (i.e., 0.05 mm) or when the total number of iterations exceeds 30.

3 Experiments and Results

The accuracy and efficiency of our approach was evaluated using 5 sets of patient dental models qualitatively and quantitatively [IRB# Pro00003644]. First, each pair of the upper and lower stone dental models were scanned separately using a cone-beam computed tomography scanner, forming a set of independent upper and lower digital models in STL format. The models are reconstructed by standard marching cubes and Laplacian-based surface smoothing. Each model contains about 700 thousand triangles (1.8 million vertices). The quality of the models is adequate in CASS practice for designing surgical splints. Next, the final occlusion of the upper and lower stone models were hand-articulated by two experienced orthodontists, and scanned together using the same scanner, forming a final occlusal template. The corresponding individually scanned models were then registered to the template, resulting in the upper and lower teeth at their final occlusion (control group – the ground truth). Third, our three-stage approach was used to automatically articulate the upper and lower models to the final occlusion (experimental group). The code was written using Matlab and run on a regular office personal computer (i7 CPU and 16GB memory). Finally, the computer-generated occlusions were compared to the hand-articulated ones.

During the qualitative evaluation, the corresponding computer- and hand-articulated dental models were randomly assigned as the first or second set. Two orthodontists, blinded from the articulation method, together evaluated results on a 27” monitor. A 3-scale visual analog scale (VAS, 1: the first set was better; 2: they were equal; and 3: the first set was worse) was used. The evaluation criteria included: midline alignment, Class I canine relation, Class I molar relationship, and maximum contact. During the quantitative evaluation, we calculated the distances of midline and canines deviating from their ideal positions along their local x-

axis using corresponding midline and canine key landmarks (Table 1). We also calculate the *Euclidian* distances between molar key landmarks. Finally, Wilcoxon Signed Rank tests were performed.

The results showed that all the upper and lower dental models were successfully aligned to the desired final occlusion using our approach. The computational time for each set of the articulation was within 3 minutes. The qualitative results showed that all 5 sets of computer-articulated models were as good as the hand-articulated ones (Fig. 3). The quantitative results showed that except one, there was no statistically significant difference between the computer- and hand-articulated final occlusions. The distance of the left molar relationship generated by our approach was statistically smaller than the ground truth, indicating the computer-generated occlusions were better than the hand-articulated ones (Table 2).

4 Discussion and Conclusion

Previously proposed methods of digital dental articulation either were ineffective, convoluted, or required labor-intensive interaction. Our proposed three-stage approach is able to effectively, accurately and full automatically articulate the upper and lower teeth into a desired final dental occlusion for one-piece maxillary orthognathic surgery. In the first stage, the POI of occlusal surface and four key landmarks that are not digitized in clinical routine are automatically extracted from the teeth models. In the second stage, the upper and lower teeth are aligned to fulfill a clinically desired M-C-M relationship by minimization of sum of distances between them. In the third stage, the upper and lower teeth are finely articulated to a maximum contact with the collision and clinical criteria constraints. In the future, we will validate the approach ultimately using a larger sample size. We will also expand our approach to multi-piece maxillary orthognathic surgery.

Acknowledgment

This work was supported in part by NIH grants (R01 DE022676 and R01 DE027251).

References

1. Xia JJ, et al., Algorithm for planning a double-jaw orthognathic surgery using a computer-aided surgical simulation (CASS) protocol. Part 1: planning sequence. International journal of oral and maxillofacial surgery, 2015 44(12): p. 1431–1440. [PubMed: 26573562]
2. Nadjmi N, et al., Virtual occlusion in planning orthognathic surgical procedures. International Journal of Oral & Maxillofacial Surgery, 2010 39(5): p. 457–462. [PubMed: 20226628]
3. Wu W, et al., Haptic simulation framework for determining virtual dental occlusion. International Journal of Computer Assisted Radiology and Surgery, 2017 12(4): p. 595–606. [PubMed: 27601232]
4. Chang Y-B, et al., An automatic and robust algorithm of reestablishment of digital dental occlusion. IEEE transactions on medical imaging, 2010 29(9): p. 1652–1663. [PubMed: 20529735]
5. Chang Y-B, et al., In vitro evaluation of new approach to digital dental model articulation. Journal of oral and maxillofacial surgery : official journal of the American Association of Oral and Maxillofacial Surgeons, 2012 70(4): p. 952–962.
6. Xia JJ, et al. Automated Digital Dental Articulation in Medical Image Computing and Computer-Assisted Intervention – MICCAI 2010. 2010 Berlin, Heidelberg: Springer Berlin Heidelberg.

7. Li J, et al., New approach to establish an object reference frame for dental arch in computer-aided surgical simulation. International journal of oral and maxillofacial surgery, 2017 46(9): p. 1193–1200. [PubMed: 28499508]
8. Xia JJ, et al., Algorithm for planning a double-jaw orthognathic surgery using a computer-aided surgical simulation (CASS) protocol. Part 2: three-dimensional cephalometry. International Journal of Oral & Maxillofacial Surgery, 2015 44(12): p. 1441–1450. [PubMed: 26573563]

Author Manuscript
Author Manuscript
Author Manuscript

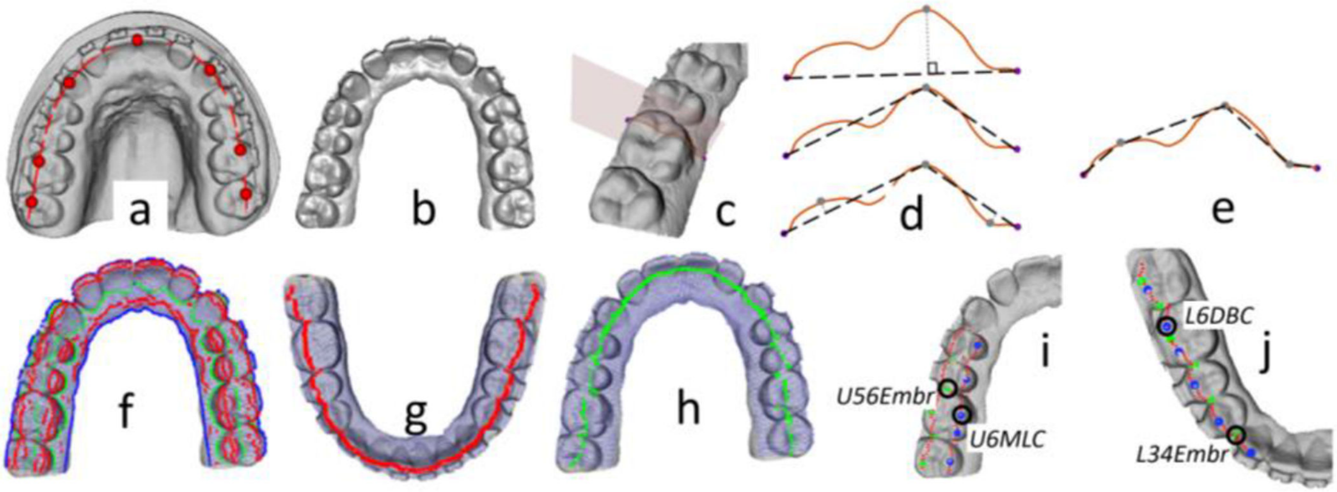

Fig. 1.
Points-of-Interest (POI) Extraction and Landmark Detection
(Note: the diameter of all the landmarks/points are intentionally enlarged for illusion purpose.)

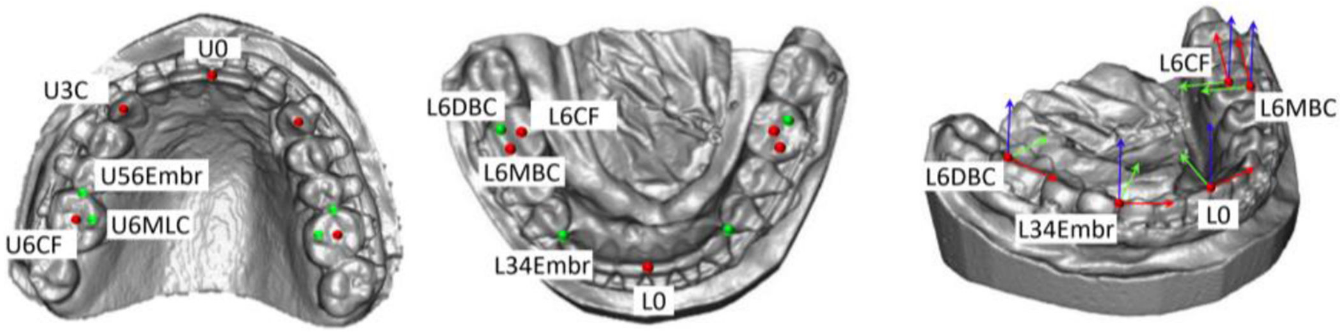

(a) Upper landmarks (red: digitized, green: detected)

(b) Lower landmarks (red: digitized, green: detected)

(c) Local coordinate system (red: *x-axis*, green: *y-axis*, blue: *z-axis*)

Fig. 2.

Landmarks and Local Coordinate Systems

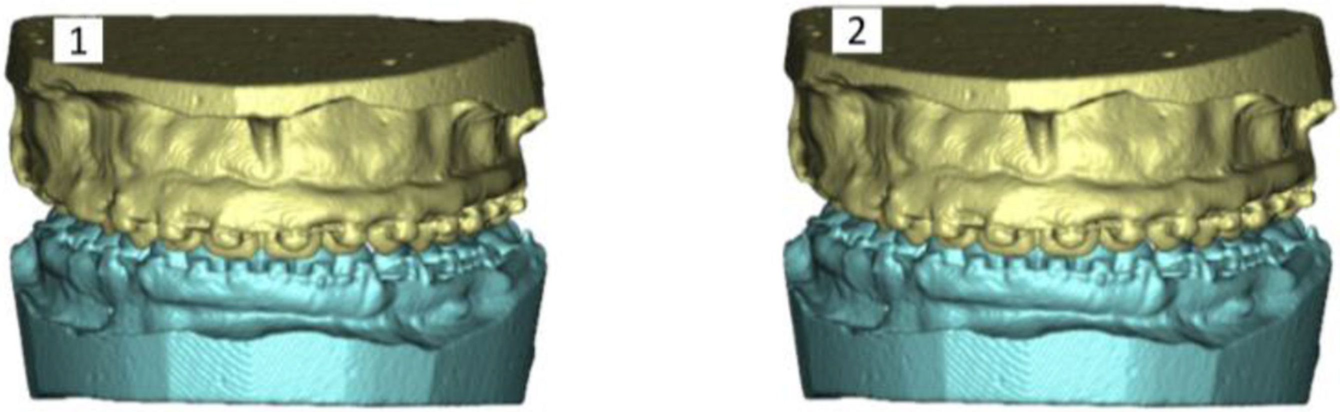

Fig. 3.
Results of a randomly selected case (1: hand-articulated; 2: computer-generated)

Table 1.

Teeth landmarks used in our proposed approach

	Upper Teeth Landmark	Predefined Name	Corresponding Lower Teeth Landmark	Predefined Name
Midline	Midpoint of central incisors	U0 [1,2]	Midpoint of central incisors	L0 [1,2]
Canine	Canine cusp	U3C [1,2]	Embrasure between canine and 1st premolar	L34Embr [2,*]
	-	-	Canine cusp	L3C [1]
Molar	Embrasure between 2nd premolar and 1st molar	U56Embr [2,*]	Mesiobuccal cusp of 1st molar	L6MBC [1,2]
	Mesiobuccal cusp of 1st molar	U6MBC [1]	-	-
	Mesiolingual cusp of 1st molar	U6MLC [2,*]	Central fossa of lower 1st molar	L6CF [2]
	Central fossa of 1st molar	U6CF [2]	Distobuccal cusp of 1st molar	L6DBC [2,*]
	Mesiobuccal cusp of 2nd molar	U7MBC [1]	-	-
	-	-	Mesiobuccal cusp of 2nd molar	L7MBC [1]

[1:] used for POI extraction;

[2:] used for M-C-M alignment;

[*] automatically detected landmark

Table 2.

Measurement Comparison

	Hand-Articulated			Computer-Articulated			
	Median	**Range**		**Median**	**Range**		**P Value**
Midline Deviation	0.04	−0.49	0.41	0.35	−0.52	0.44	0.87
Right Canine Relation	1.37	0.27	2.53	0.95	0.56	2.53	0.98
Left Canine Relation	−1.44	−1.93	−0.88	−1.23	−1.84	−0.57	0.96
Right Molar Relation	2.12	1.37	3.23	2.15	1.64	3.76	0.11
Left Molar Relation	2.87	1.91	4.38	2.35	1.64	4.11	0.02